

Journal Pre-proof

COA6 facilitates cytochrome *c* oxidase biogenesis as thiol-reductase for copper metallochaperones in mitochondria

David Pacheu-Grau, Michał Wasilewski, Silke Oeljeklaus, Christine Silvia Gibhardt, Abhishek Aich, Margarita Chudenkova, Sven Dennerlein, Markus Deckers, Ivan Bogeski, Bettina Warscheid, Agnieszka Chacinska, Peter Rehling

PII: S0022-2836(20)30102-9

DOI: <https://doi.org/10.1016/j.jmb.2020.01.036>

Reference: YJMBI 66433

To appear in: *Journal of Molecular Biology*

Received Date: 5 November 2019

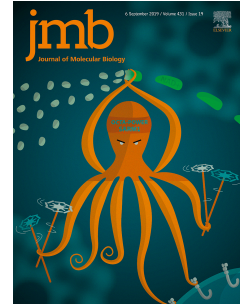
Revised Date: 23 January 2020

Accepted Date: 27 January 2020

Please cite this article as: D. Pacheu-Grau, M. Wasilewski, S. Oeljeklaus, C.S. Gibhardt, A. Aich, M. Chudenkova, S. Dennerlein, M. Deckers, I. Bogeski, B. Warscheid, A. Chacinska, P. Rehling, COA6 facilitates cytochrome *c* oxidase biogenesis as thiol-reductase for copper metallochaperones in mitochondria, *Journal of Molecular Biology*, <https://doi.org/10.1016/j.jmb.2020.01.036>.

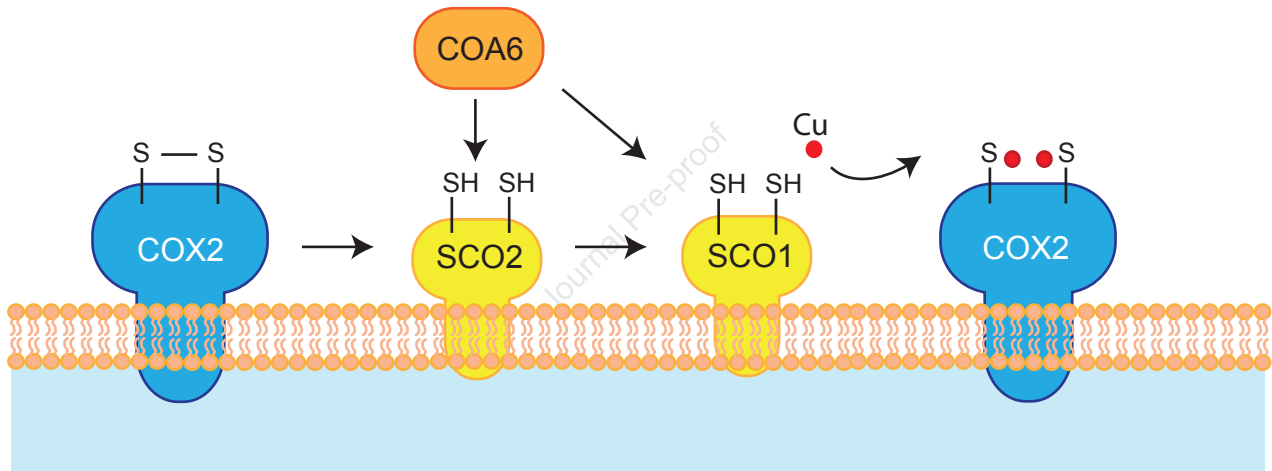
This is a PDF file of an article that has undergone enhancements after acceptance, such as the addition of a cover page and metadata, and formatting for readability, but it is not yet the definitive version of record. This version will undergo additional copyediting, typesetting and review before it is published in its final form, but we are providing this version to give early visibility of the article. Please note that, during the production process, errors may be discovered which could affect the content, and all legal disclaimers that apply to the journal pertain.

© 2020 Published by Elsevier Ltd.



Credit Author Statement

David Pacheu-Grau. Conceptualization, methodology, investigation, visualization, writing-original draft and supervision. **Michał Wasilewski.** Methodology, investigation, visualization, and writing-review/editing. **Silke Oeljeklaus.** Investigation, visualization and writing-review/editing. **Christine Silvia Gibhardt.** Investigation and writing-review/editing. **Abhishek Aich.** Investigation. **Sven Dennerlein.** Investigation and visualization. **Margarita Chudenkova.** Investigation. **Markus Deckers.** Investigation and visualization. **Ivan Bogeski.** Resources, writing-review/editing and funding acquisition. **Bettina Warscheid.** Resources, writing-review/editing and funding acquisition. **Agnieszka Chacinska.** Conceptualization, resources, writing-review/editing and funding acquisition. **Peter Rehling.** Conceptualization, resources writing-original draft, project administration, funding acquisition and supervision.



COA6 facilitates cytochrome c oxidase biogenesis as thiol-reductase for copper metallochaperones in mitochondria

David Pacheu-Grau^{1,#}, Michał Wasilewski^{2,3}, Silke Oeljeklaus^{4,5}, Christine Silvia Gibhardt⁶, Abhishek Aich¹, Margarita Chudenkova¹ Sven Dennerlein¹, Markus Deckers¹, Ivan Bogeski⁶, Bettina Warscheid^{4,5}, Agnieszka Chacinska^{2,3}, & Peter Rehling^{1,7,#}

¹Department of Cellular Biochemistry, University Medical Center Göttingen, D-37073 Göttingen, Germany.

² Laboratory of Mitochondrial Biogenesis, Centre of New Technologies, University of Warsaw, Warsaw, Poland.

³ ReMedy International Research Agenda Unit, Centre of New Technologies, University of Warsaw, Poland.

⁴ Biochemistry and Functional Proteomics, Institute of Biology II, Faculty of Biology.

⁵ Signalling Research Centres BLOSS and CIBSS, University of Freiburg, D-79104 Freiburg, Germany.

⁶ Molecular Physiology, Institute of Cardiovascular Physiology, University Medical Center, Georg-August-University, Göttingen, Germany.

⁷ Max-Planck Institute for Biophysical Chemistry, D-37077, Göttingen, Germany.

Correspondence: Peter Rehling, Department of Cellular Biochemistry, University Medical Center Göttingen, Humboldtallee 23, 37073 Göttingen, Germany.

Fax: +49 551 395979;

Tel: +49 551 395947;

Email: peter.rehling@medizin.uni-goettingen.de

David Pacheu-Grau, Department of Cellular Biochemistry, University Medical Center Göttingen, Humboldtallee 23, 37073 Göttingen, Germany.

Fax: +49 551 395979;

Tel: +49 551 394571;

Email: David.Pacheu-Grau@med.uni-goettingen.de

Abstract

The mitochondrial cytochrome *c* oxidase, the terminal enzyme of the respiratory chain, contains heme and copper centers for electron transfer. The conserved COX2 subunit contains the Cu_A site, a binuclear copper center. The copper chaperones SCO1, SCO2, and COA6 are required for Cu_A center formation. Loss of function of these chaperones and the concomitant cytochrome *c* oxidase deficiency cause severe human disorders. Here we analyzed the molecular function of COA6 and the consequences of COA6 deficiency for mitochondria. Our analyses show that loss of COA6 causes combined complex I and complex IV deficiency and impacts membrane potential driven protein transport across the inner membrane. We demonstrate that COA6 acts as a thiol-reductase to reduce disulphide bridges of critical cysteine residues in SCO1 and SCO2. Cysteines within the CX₃CX_NH domain of SCO2 mediate its interaction with COA6 but are dispensable for SCO2-SCO1 interaction. Our analyses define COA6 as thiol-reductase, which is essential for Cu_A biogenesis.

Keywords: mitochondria, cytochrome c oxidase, Cu_A center, COA6, copper metallochaperones

Journal Pre-proof

Introduction

Mitochondria fulfil central functions in eukaryotic metabolism. In addition to participating in metabolite turnover and synthesis, mitochondria supply cells with the bulk of energy to drive cellular processes. At the heart of this process is the oxidative phosphorylation system (OXPHOS), which is located in the inner mitochondrial membrane. The protein complexes of the OXPHOS system derive from subunits of dual genetic origin. Thirteen subunits are encoded on human mitochondrial DNA (mtDNA), whereas the rest of the components are encoded in the nucleus, synthesized on cytosolic ribosomes, and transported into mitochondria [1,2]. Hence, biogenesis of respiratory chain complexes and the F_1F_0 ATP synthase requires assembly of proteins that reach the inner membrane through different supply routes [3,4]. In addition, during the assembly process the redox-active cofactors need to be integrated. The cytochrome *c* oxidase (complex IV) contains two heme cofactors (a and a_3) and two copper centers (Cu_A and Cu_B), required for reduction of molecular oxygen to water.

COA6 represents a conserved complex IV assembly factor required for the metalation of the COX2 subunit, which is critical for the formation of the Cu_A center in the intermembrane space domain [5-10]. Loss of COA6 function is associated with hypertrophic cardiomyopathy and loss of either complex I and IV [11] or isolated complex IV deficiency [12]. COA6 was found in a complex with the metallochaperones SCO1 and SCO2, which are required for copper insertion into the Cu_A center [7,8] (Fig 1A). SCO1 and SCO2 have distinct but cooperative functions in copper delivery to the Cu_A . While SCO2 is thought to deliver the copper molecule to COX2, SCO1 facilitates copper transfer to SCO2 from COX17 [13,14]. In addition, SCO2 is considered to regulate the thiol redox or metalation state of SCO1, thereby fulfilling a signalling role to regulate cellular copper efflux [15]. In contrast, recent *in*

vitro studies suggested that copper transfer to the Cu_A site only requires SCO1, while SCO2 regulates the thiol redox state of COX2 but not of SCO1 [16]. Since cofactor insertion into the Cu_A center is thought to be coupled to COX2 insertion into the membrane, SCO1 and SCO2 have been found to interact with FAM36A [17]. In addition SCO1, SCO2 and COA6 have been found to interact with COX16, a factor involved in delivering COX2 after metalation to the complex IV assembly intermediates (MITRAC complexes) [18]. A structural analysis of Coa6, revealed that the four Cys of the CX₉C-CX₁₀C motive form disulphide bridges. Based on the observation, that the Cys₅₈-Cys₉₀ disulphide bridge could be chemically reduced to free thiol groups, has been taken as indication that these residues could be required for copper coordination [19]. However, the molecular function of COA6 in copper insertion into the Cu_A center and the question as to how the structural determinants of the protein relate to its molecular function remain unaddressed.

Here, we generated a COA6 knock out HEK 293T cell line to analyze COA6 function in Cu_A-site formation. Loss of COA6 function led to combined complex I and complex IV deficiency. A concomitant reduction of the inner membrane potential ($\Delta\Psi$) caused defects in membrane potential driven protein transport across the inner mitochondrial membrane, whereas the Mitochondrial intermembrane space import and assembly protein 40 (MIA40/ CHCHD4)-dependent import into the intermembrane space was not compromised. Our analyses demonstrated that COA6 acts as a thiol-reductase to reduce disulphide bridges in the metallochaperones SCO1 and SCO2. The cysteines of the thioredoxin-like fold of SCO2 are required for the interaction with COA6 but dispensable for the dynamic interaction between SCO1 and SCO2. We conclude that the thiol reduction activity of COA6 is necessary for proper copper transfer to the Cu_A site.

Journal Pre-proof

Results

Lack of COA6 affects complex I and complex IV

COA6 participates in copper insertion into COX2 through interactions with the copper chaperones SCO1 and SCO2 and the assembly factors COX18 and COX16 ([7,8,10,18]). However, the mechanism of copper transfer to COX2 and the role of COA6 in this process are ill defined. To understand COA6 function in this process, we generated a COA6 knock out HEK 293T cell line (COA6^{KO}) using the CRISPR/Cas9 system. Sequencing analyses revealed a deletion in Exon 2 that generates a premature Stop codon in the COA6 gene (Fig. Sup1A). The COA6^{KO} displayed a strongly reduced growth rate compared to the wild type. Introduction of a FLAG-tagged COA6 version into the knock out partially restored cellular growth (Fig. 1B). Since patients carrying COA6 mutations displayed fatal hypertrophic cardiomyopathy and presented in one case with combined complex I and complex IV [11] and in another case with isolated complex IV deficiency [12], we assessed respiratory chain function in the mutant cells. Therefore, we measured oxygen consumption by real time respirometry in intact cells. Respiration of COA6 knock out cells was drastically reduced compared to the wild type in agreement with a defect of oxidative phosphorylation (Fig. 1C). To define how loss of COA6 affected the different complexes of the respiratory chain, we measured the activity and amounts of the cytochrome c oxidase. Complex IV activity and amount were drastically reduced in COA6 knock out cells as expected. Expression of a FLAG-tagged COA6 largely restored this defect (Fig. 1D and E) and in Western blot analyses was also found to rescue steady state proteins levels of complex IV components (Fig. Sup1B). We previously showed that silencing of COA6 by siRNA treatment also led to reduced activity and amounts of complex I [7]. In contrast, Stroud et al. reported that the loss of COA6 led to selective complex IV deficiency [8]. Therefore, we

investigated if complex I was affected in COA6^{KO} cells. To this end, we determined the enzymatic activity of complex I in a colorimetric assay. Interestingly, compared to wild type, the activity of complex I was strongly decreased in COA6^{KO} cells (Fig. 1F). Under certain conditions, defects in oxidative phosphorylation can cause production of reactive oxygen species (ROS)[20] and thus affect the mitochondrial glutathione redox potential. To address this, we measured superoxide production in wild type and COA6^{KO} cells using the fluorescent dye MitoSOX. As depicted in (Fig. 1G) we found a decrease in superoxide levels in the absence of COA6. In addition, we analyzed the general redox buffering capacity of mitochondria by measuring glutathione redox potential using the Grx1-roGFP2 sensor targeted to the intermembrane space (IMS) or the mitochondrial matrix. These fluorescent sensors monitor the glutathione redox potential that is affected by ROS [21]. These analyses showed no differences of the redox potential between wild type and COA6^{KO} cells (Fig. 1H). Accordingly, loss of COA6 leads to a combined complex IV and complex I deficiency in mitochondria. However, an increase in ROS production was not apparent in mutant cells nor did we detect alterations in the mitochondrial glutathione redox potential.

Lack of COA6 impacts protein import

To address to which extent the different components of complexes I and IV were altered in the absence of COA6 and if other mitochondrial proteins were also affected, we assessed changes in the proteome of mitochondria isolated from wildtype and COA6-deficient cells by quantitative mass spectrometry. Interestingly, the mitochondrial-encoded core components of cytochrome *c* oxidase COX1, COX2, and COX3 were strongly decreased in COA6^{KO} mitochondria. In addition, other structural components of complex IV and of complex I were decreased in

mitochondria in the absence of COA6. In contrast, constituents of complex V were not significantly affected (Fig. 2A). These results were confirmed using SDS-PAGE and Western blotting (Fig. 2B). However, to our surprise, many other mitochondrial proteins not related to the OXPHOS system were decreased in COA6^{KO} mitochondria. We reasoned that a reduced activity of the respiratory chain would impact the transfer of protons to the intermembrane space and thereby affect the mitochondrial inner membrane potential, which drives protein import into mitochondria. To this end, we measured the membrane potential by flow cytometry. COA6^{KO} cells indeed displayed a strongly reduced membrane potential (Fig. 2C). Accordingly, it is conceivable that the loss of complexes I and IV and the resulting decrease of the inner membrane potential reduced the import capacity of mitochondria leading to alterations in protein abundance. Therefore, we imported radiolabeled precursor proteins that follow different import routes into purified COA6^{KO} mitochondria. The presequence-containing precursors OTC (ornithine-transcarbamylase) and Su9-DHR (subunit 9 of the F₁F₀ ATP synthase) are transported by the TIM23 complex in a membrane potential-dependent manner into the mitochondrial matrix. Compared to wild type mitochondria, the import of both precursor proteins was reduced in the absence of COA6 (Fig. 2D and E). Metabolite carriers are imported and inserted into the inner mitochondrial membrane by the TIM22 complex in a membrane potential dependent manner. We performed *in vitro* import analyses of the model carrier transport pathway substrate ANT3 (ADP/ATP carrier 3) and SLC25A19 (thiamine pyrophosphate carrier). After import, mitochondria were solubilized and imported proteins analyzed by Blue Native PAGE (BN-PAGE). In both cases, we observed a strongly decreased import in COA6^{KO} mitochondria (Fig. 2F and G). In contrast to presequence-containing precursors and carriers, mitochondrial proteins of the intermembrane space that contain twin CX_NC

motifs, which are oxidized upon import forming disulphide bridges with the assistance of MIA40, are imported independent of a membrane potential. Hence, we analyzed the import efficiency of the MIA40 substrates COX6B1 and COX19 in the absence of COA6. Interestingly, import of precursors into the intermembrane space along the MIA40 pathway was not impaired in the absence of COA6 but rather accelerated (Fig. 2H and I). In summary, in the absence of COA6, the import routes that depend on the inner membrane potential are affected. However, the membrane potential independent import into the intermembrane space via MIA40 was not reduced but rather stimulated. Hence, a loss of membrane potential due to loss of complexes I and IV causes pleiotropic defects via compromised import of proteins that translocate across the inner membrane.

Cysteines in the CXXXC motif of SCO2 are required for binding to COA6

COA6 cooperates with SCO1 and SCO2 in the metalation of COX2 [7,8]. Mimicking pathologic mutations in either COA6 or SCO2 affected co immunoisolation of these proteins [7]. To address if SCO2 and COA6 directly interacted with each other, we incubated COA6^{FLAG} containing mitochondria with the sulfhydryl reactive crosslinker BMH. After FLAG immunoisolation, COA6-SCO2 crosslinks were recovered in the eluate, indicating that both proteins were covalently linked via crosslinking of cysteine residues (Fig 3A).

SCO1 and SCO2 contain a CX₃CX_nH motif that allows them either to bind Cu(I) with high affinity or to act as thiol-oxidoreductases [22,23]. Therefore, we analyzed the relevance of the cysteines of the CX₃CX_nH motif for the interaction with COA6 and consequently for the dynamics of the copper transfer reactions. To this end, we generated cysteine mutants of SCO2. SCO2 contains three cysteines (C₁₁₅, C₁₃₃, and C₁₃₇), with C₁₃₃ and C₁₃₇ being part of the CX₃CX_nH motif. We generated

single mutants changing cysteine to serine residues (SCO2^{C115S}, SCO2^{C133S}, SCO2^{C137S}) (Fig. 3B). In order to analyze the effect of the cysteine mutants, we generated radiolabelled versions of wild type, SCO2^{C115S}, SCO2^{C133S}, and SCO2^{C137S}. SCO2 could be efficiently import into purified wild type mitochondria in a membrane potential-dependent manner. Upon import SCO2 was processed to the mature form (Fig.3C). Similarly, the mutant versions of SCO2 were efficiently imported into wild type mitochondria (Fig. 3D). To analyze how the cysteine mutants in SCO2 affected the interaction with COA6, we performed *in vitro* import of radiolabelled versions of SCO2 into isolated mitochondria from cells expressing C-terminally FLAG-tagged COA6. After import, COA6 was immunisolated and bound SCO2 detected by autoradiography. Wild type SCO2 (SCO2^{WT}) efficiently co-precipitated with COA6^{FLAG} after *in vitro* import. SCO2^{C115S} (not being in close proximity to the copper coordination center) interacted with COA6^{FLAG} in similar amounts as wild type SCO2. Interestingly, the SCO2^{C133S} and SCO2^{C137S} mutants, which are affected in the CX₃CX_nH motif, displayed drastically decreased interactions with COA6^{FLAG} by about 80% (Fig. 3E). Thus, the cysteines of the CX₃CX_nH motif are important for SCO2/COA6 interaction. Therefore, we addressed if COA6 and SCO2 directly interacted through disulphide bridge formation. For this we treated samples with Cu²⁺ as a redox catalysts to oxidize free sulfhydryls and to form disulfide bonds between cysteine residues in proximity to each other. After immunisolation of COA6^{FLAG}, we observed specific adducts detected by both SCO2 and FLAG antisera (Fig 3 F).

SCO1 and SCO2 cooperate in the delivery of copper to the cytochrome *c* oxidase subunit COX2 [14]. To analyze if the cysteines in SCO2 determined not only the interaction with COA6 but also the dynamics of SCO1 and SCO2, we performed *in vitro* import of radiolabelled versions of SCO2 into mitochondria isolated from cells

expressing FLAG-tagged SCO1. Interestingly, the interaction between SCO1 and the fully imported, mature SCO2^{C137S} was similar to that of wild type SCO2 (Fig.3G). Accordingly, the CX₃CX_nH motive of SCO2 was not relevant for the SCO1/SCO2 interaction. Thus, it is tempting to speculate that the SCO1/SCO2 interaction does not occur through disulphide bridge formation. However, based on these observations, it is likely that a COA6/SCO2 complex forms disulphide bridges during the copper transfer cycle.

COA6 acts as a thiol-reductase for copper metallochaperones SCO1 and SCO2

SCO2 has been shown to reduce cysteines residues in the copper coordination site of COX2 *in vitro*, whereas it was unable to oxidize cysteines in SCO1, implying that other factors are involved in these redox reactions in mitochondria [16]. Our analyses showed that the cysteines present in the CX₃CX_nH motive in SCO2 are determinants for the interaction with COA6. Therefore, we considered the possibility that COA6 might be involved in the regulation of the redox state of the copper metallochaperones during Cu_A biogenesis. To address this, we analyzed the redox state of cysteines in SCO2 in COA6^{KO} mitochondria using a maleimide derivate coupled to a DNA probe. Upon reaction of the probe with a free cysteine, the target protein shows an apparent size shift of approx. 14 kDa in SDS-PAGE analysis. In wild type mitochondria SCO2 displayed a molecular weight shift corresponding to three free thiol groups. In contrast, in COA6^{KO} mitochondria, SCO2 accumulated in a state corresponding to a single reduced cysteine (Fig. 4A). A quantitative assessment of the ratio between reduced and oxidized form of SCO2 revealed a drastic shift towards the oxidized state in mitochondria lacking COA6. To address if the oxidized form of SCO2 in COA6^{KO} mitochondria represented a form with disulphide bridge, we pre-incubated COA6^{KO} mitochondria with DTT prior to the

maleimide-mediated modification. Upon chemical modification of DTT treated COA6^{KO} mitochondria, SCO2 displayed a wild type like migration pattern (Fig. 4A and B). To analyze if COA6 contributed to the oxidative state of SCO1 *in organello*, we assessed the availability of free cysteines by maleimide modification analyses in mitochondria lacking COA6. While a shifted form of SCO1 that corresponded to two free thiol groups was apparent in wild type mitochondria, COA6^{KO} mitochondria displayed an accumulation of non-modified SCO1, implying that the two cysteines were oxidized. The quantification of the ratio of reduced and oxidized SCO1 showed again a drastic decrease of the oxidized state in the absence of COA6 (Fig. 4C). Upon treatment of COA6^{KO} mitochondria with DTT, SCO1 could be fully reduced and thus be modified by the maleimide (Fig. 4C and D). To support the specificity of the observed redox phenotype upon lack of COA6, we expressed a FLAG-tagged version of COA6 in COA6^{KO} cells. The redox phenotype of SCO1 and SCO2 in COA6^{KO} cells could be rescued by expression of COA6 (Fig. 4E and F), confirming that COA6 is required for reduction of the disulphide bridges in both proteins. In summary, our findings showed that COA6 is required to reduce a disulphide bridge in both SCO1 and SCO2 and that this effect is not indirectly caused by increased ROS production or an altered redox state of the intermembrane space.

Discussion

The catalytic core of the cytochrome *c* oxidase is conserved from bacteria to human. The formation of the binuclear copper center Cu_A is therefore a common process and the particular high reactivity of copper ions necessitates that the copper delivery is assisted by copper metallochaperones. However, the mechanisms of Cu_A biogenesis differ between organisms with regard to the participating copper-binding proteins. In bacteria, the activity of a periplasmic thioredoxin-like reductase TlpA maintains the

active site cysteine pairs of CoxB and Scol in the reduced state and is thus required for Cu^{2+} binding. The copper chaperone Scol reacts with apo-CoxB to establish a stable Cu^{2+} containing complex, which is released to form a CoxB- Cu^{2+} with the aid of the chaperone PcuC. A second round of PcuC action delivers Cu^+ to CoxB, forming the Cu_A center [24]. In human mitochondria, other players among these COA6 have been identified as members of the copper insertion machinery for COX2 [7,8]. Interestingly, mammalian mitochondria lack a TlpA homolog. Therefore, the required thiol-reductase activity has to be a function of either SCO1, SCO2, or COA6. Our findings suggest that COA6 shows a thiol-reductase activity and is involved in the reduction of cysteines in the $\text{CX}_3\text{CX}_n\text{H}$ motif of SCO1 and SCO2. Whereas SCO1 has been shown to transfer copper to COX2 *in vitro* in a two-step reaction, SCO2 presented a thiol-reductase activity that was able to reduce cysteinyl sulfurs of COX2 in a copper bound state [16]. Based on these observations, we propose that COA6 recycles SCO2 cysteines into a redox-active form, enabling further rounds of COX2 cysteinyl sulfur reduction. Remarkably, SCO2 reduced thiol groups of Apo-COX2 at a 2:1 stoichiometry *in vitro* [16]. Since COA6 cooperates with SCO2 during COX2 metallation, it is plausible that *in vivo* COA6 and SCO2 each provide one reducing equivalent per one COX2 molecule. Indeed, the redox potential of yeast COA6 ($-349 \pm 1 \text{mV}$) [19] indicated that COA6 could reduce the disulphide bonds in COX2 ($-288 \pm 3 \text{mV}$) [16], SCO2 (less than -300mV) [25] or SCO1 ($-277 \pm 3 \text{mV}$) [26]. However, the ability of COA6 to reduce thiol groups of COX2 *in vivo* could not be addressed in our model system, since cells lacking COA6 lack detectable levels of COX2. In addition, our analysis suggests that COA6 is involved in SCO1 reduction. *In vitro*, SCO1 can receive copper atoms from COX17 independently of the redox state of its cysteine. Whereas SCO2 necessarily needs to be in a reduced state to receive copper, SCO1 can be either in a reduced state or it can be in an oxidized state,

being reduced by COX17 in a simultaneous step with copper transfer [27]. However, it is also conceivable that prior to copper transfer by COX17, SCO1 may be reduced by COA6. During revision of this manuscript, Soma et al solved the structure of human COA6 and showed in *in vitro* analyses that COA6 was able to reduce cysteine residues in purified SCO1, SCO2, and COX2. These results, support our analyses of COA6 acting as a thiol-reductase *in vivo*. However, using COA6 patient-derived cells, they could only observed effects on cysteine oxidation of SCO1 but not SCO2. Differences in the cellular models used for investigation may account for this difference with our analyses and need to be further studied in the future [28].

In conclusion, our results provide insights into the mechanistics of Cu_A biogenesis and defines the function of COA6 as a thiol-reductase for copper metallochaperones. In addition, we demonstrate that the loss of COA6 not only affects complex IV assembly but also the formation of respiratory chain complex I. Remarkably, only one of the patients described with COA6 mutations showed a decreased complex I activity [11] [12]. The COA6 knock out mutant used here displays reduced complex I and IV activity. However, at this point the question as to how a loss of COA6 affects complex I remains open as no link between copper chaperone activity and complex I biogenesis has been observed.

Our analyses indicate that that loss of OXPHOS activity and the concomitant reduction of the membrane potential indirectly influences the mitochondrial proteome through protein import defects. Interestingly, the $\Delta\psi$ -independent import of substrates along the MIA40 pathway was not decreased but rather increased in the absence of COA6. Upregulation of mitochondrial import pathways has been frequently shown when one import pathway is defective [29-31]. However, the molecular reason behind this phenomenon remains unclear. In addition, other additional mechanisms apart from reduced membrane potential may contribute to the altered mitochondrial

proteome in COA6^{KO} cells. For instance, alteration of copper homeostasis drastically alters the Fe/S cluster formation that involves the mitochondrial ISCA1/2 and GLRX5 proteins [32]. Interestingly, the protein levels of ISCA2 and to lesser extent those of GLRX5 are decreased in the absence of COA6 (see Sup table 1). Thus, it is conceivable that impaired iron-sulfur cluster biogenesis affects may impact the steady state levels of different mitochondrial protein and thereby cause alterations in protein abundance in many mitochondrial functions in addition to the respiratory chain e.g. citric cycle, heme biosynthesis, lipoic acid synthesis. Accordingly, COA6 dysfunction, e.g. in COA6 patients, leads to pleiotropic defects in mitochondrial function.

Material and Methods

Cell Culture, Generation of Cell lines and Proliferation Assay.

HEK293T Flp-In™ T-REX™ or HEK293 were cultured in DMEM media, supplemented with 10% (v/v) FBS, 2 mM L-glutamine, 1 mM sodium pyruvate and 50 µg/mL uridine at 37 °C under a 5% CO₂ humidified atmosphere. The COA6^{KO} HEK293T cell line was generated using CRISPR-Cas9 genome editing as previously described [33]. Briefly, specific sgRNA were designed to target all isoforms of COA6. Oligonucleotides were then annealed and ligated into the pX458 vector, which contains GFP. Cells were transfected and sorted into single wells of a 96-well plate. Clones were screened for the absence of COA6 by immunoblotting. 1 clone was used for further analysis and sequencing after genomic DNA isolation confirmed disruption of the COA6 gene. Rescue cell line expressing C-terminally tagged generated using HEK293T Flp-In™ T-REX™ as previously described [18]. Cell lines stable expressing C-terminally FLAG tagged versions of COA6 and SCO2 were generated using HEK293T Flp-In™ T-REX™ during previous studies[7]. C-terminally FLAG tagged SCO1 was generated amplifying SCO1 (NM_004589.4) from cDNA and incorporating FLAG sequence in the reverse primer. Amplicon was cloned into pcDNA5/FRT/TO vector and HEK293T Flp-In™ T-REX™ cells were transfected and selected as previously described [34]. For SILAC analysis, cells were grown for five passages on DMEM medium lacking arginine and lysine, supplemented with 10% (v/v) dialyzed fetal bovine serum, 600 mg/l proline, 42 mg/l arginine hydrochloride (¹³C₆, ¹⁵N₄-arginine in 'heavy' media), and 146 mg/l lysine hydrochloride (¹³C₆, ¹⁵N₂-lysine in 'heavy' media) (Cambridge Isotope Laboratories, Tewksbury, MA, USA).

Cell proliferation experiments were performed by seeding 250000 cells in 6 well-plates. After 72h hours, cells were recovered in PBS and counted using an automated cell counter Countess™ (Invitrogen).

Real-time respirometry

Oxygen consumption rate (OCR) was measured with a XF96 Extracellular Flux Analyzer (Seahorse Bioscience, Billerica, MA, USA). HEK293T cells were seeded the day of the measurement at a density of 40.000 cells/well. Baseline respiration was measured in DMEM supplemented with 1 mM pyruvate and 25 mM galactose after calibration at 37 °C in an incubator without CO₂. Periodic measurements of oxygen consumption were performed and OCR was calculated from the slope of change in oxygen concentration over time. Metabolic states were measured after subsequent addition of 3 μM oligomycin, 1 μM carbonyl cyanide 4 (trifluoromethoxy)phenylhydrazone (FCCP), 1 μM antimycin A, and 2 μM rotenone.

Enzymatic activities

A quantitative method (ELISA) for cytochrome *c* oxidase (CIV) specific activity and quantity of complex determinations (Abcam) was applied using manufacturer's instructions as previously described [35]. The lack of a negative slope due to Cytochrome *c* oxidation was consider as a complete lack of cytochrome *c* oxidase activity and set to 0. In the same way, Complex I activity measurements were performed according to manufacturer's instructions (Abcam), as previously published [7].

Membrane Potential and ROS measurements.

For estimation of membrane-potential of the mitochondria, cells were stained with 200 μ M JC-1. The values of the two fluorescence readings gave a ratiometric comparison of mitochondrial membrane potential. Further, cells were also stained with 3 μ M MitoSox Red for measuring mitochondrial ROS. In each case, 5 $\times 10^5$ cells were stained with the respective dyes for 15 min at 37°C, washed twice with 1xPBS and then measured by flow cytometry.

Flow cytometric analyses were carried out using the BD-Canto flow cytometer (Becton Dickinson). 10,000 gated events were captured and FACS-Diva software was used to compute the numeric data.

Redox potential measurements

For measuring Glutathione redox potential, WT or COA6^{KO} cells (100,000 - 300,000) were seeded on 25 mm round glass coverslips 24 – 48 h before transfection. Genetically encoded protein sensors were transfected using Fugene® HD (Promega GmbH, Mannheim, Germany) along with 1 μ g of plasmid DNA, according to the manufacturer's instructions. Imaging was performed 24 h after transfection. Plasmids pLPCX-mito-Grx1-roGFP2 and pLPCX-IMS-Grx1-roGFP2 were kindly provided by Dr. Tobias P. Dick, Heidelberg, Germany.

Imaging was performed 24 h after transfection using an inverted Olympus IX83 microscope, equipped with a MT20 Mercury-Xenon light source, CellSense Dimension software (Olympus) and a 40 \times air objective (UPlanSApo 40x 0.95, Olympus). Measurements were performed at room temperature in Ringer's buffer (pH 7.4) containing 145 mM NaCl, 4 MgCl₂, 10 mM Glucose, 10 mM HEPES, 2 mM MgCl₂ and 0.25 mM CaCl₂. The exposure time for both fluorescent channels was kept constant during the whole experiment. Excitation filters 405/20 and 470/40 were

combined with a dualband CFP/YFP emission filter (F58-017). Data are presented as background corrected fluorescence ratios of $F_{405\text{ nm}} / F_{470\text{ nm}}$.

Mitochondrial Isolation

Mitochondria used for Western blotting purposes were isolated by differential centrifugation as previously described [36]. For import experiments, mitochondria were isolated as previously described [37]. Briefly, cells were harvested and resuspended in ice-cold isotonic buffer (10 mM MOPS [pH 7.2], 75 mM mannitol, 225 mM sucrose, and 1 mM EGTA) supplemented with 2 mg/ml BSA and 2 mM PMSF, and subjected to centrifugation at $1,000 \times g$ for 5 min at 4°C. The cell pellet was then resuspended in cold hypotonic buffer (10 mM MOPS [pH 7.2], 100 mM sucrose, and 1 mM EGTA) and incubated on ice for 5–7 min. The cell suspension was homogenized in a Dounce glass homogenizer (Sartorius). Cold hypertonic buffer (1.25 M sucrose and 10 mM MOPS [pH 7.2]) was added to the cell homogenate (1.1 ml/g of cells). The homogenate was subjected to centrifugation at $1,000 \times g$ for 10 min at 4°C to pellet the cellular debris. The supernatant that contained mitochondria was then carefully aspirated and centrifuged again. The supernatant was then subjected to high-speed centrifugation at $10,000 \times g$ for 10 min at 4°C to pellet mitochondria. The pellet was resuspended in isotonic buffer without BSA and quantified using the Bradford assay.

Quantitative mass spectrometry and data analysis

Mitochondrial fractions isolated from differentially SILAC-labeled cells were mixed in a 1:1 ratio. Proteins were precipitated using acetone and resuspended in 8 M urea/10 mM ammonium bicarbonate (AmBic). Cysteine residues were reduced and alkylated by consecutive incubation with 5 mM tris(2-carboxyethyl)-phosphine/10 mM

AmBic (30 min at 37°C) and 55 mM iodoacetamide/10 mM AmBic (45 min at room temperature in the dark). Urea concentration was adjusted to a final concentration of 2 M using 50 mM AmBic and trypsin was added (1/30 protease-to-protein ratio) for proteolytic digestion overnight at 37°C. The experiment was performed in two individual replicates.

Peptide mixtures were analyzed on an Orbitrap Elite mass spectrometer coupled to an UltiMate 3000 RSLCnano HPLC system (Thermo Scientific), which was equipped with nanoEase™ M/Z Symmetry C18 pre-columns (length, 20 mm; inner diameter, 180 µm) for washing and preconcentration of the peptides and a nanoEase™ M/Z HSS C18 T3 analytical column (length, 250 mm; inner diameter, 75 µm; particle size, 1.8 µm; packing density, 100 Å) (Waters) for peptide separation. The solvent system for peptide elution consisted of 4% (v/v) dimethyl sulfoxide/0.1% (v/v) formic acid (solvent A) and 30% (v/v) acetonitrile/48% (v/v) methanol/4% (v/v) dimethyl sulfoxide/0.1% (v/v) formic acid (solvent B). Peptides were eluted by applying a gradient of 3 - 60% solvent B in 305 min, 60 - 95% B in 25 min and 5 min at 95% B at a flow rate of 300 nl/min.

The Orbitrap Elite was operated in data-dependent mode. Survey scans ranging from m/z 370 - 1700 were acquired in the orbitrap at a resolution of 120,000 (at m/z 400) with an automatic gain control (AGC) of 1×10^6 ions and a maximum injection time (IT) of 200 ms. The 25 most intense multiply charged precursor peptides were selected for low energy collision-induced dissociation in the linear ion trap applying a normalized collision energy of 35%, an activation q of 0.25, an activation time of 10 ms, an AGC of 5×10^3 , and a maximum IT of 150 ms. Dynamic exclusion of previously fragmented precursor peptides was set to 45 sec.

Mass spectrometric raw data were processed using MaxQuant/Andromeda (version 1.5.5.1; [38,39] and searched against the Uniprot human proteome set

including isoforms (downloaded December 2017) using default settings, except that the number of unique peptides and ratio counts required for protein identification and quantification, respectively, was set to one. Arg10 and Lys8 were selected as heavy labels. Carbamidomethylation of cysteine residues was set as fixed modification and methionine oxidation and acetylation of protein N-termini were considered variable modifications. The option "Requantify" was enabled to allow for the calculation of SILAC ratios even if only the isotope-labeled or unlabeled variant of a peptide is present in a sample by assigning a peptide intensity for the missing counterpart from the background signals in MS spectra at the expected m/z value. Information about proteins identified and COA6^{KO}/WT SILAC ratios determined by MaxQuant are provided in Supplemental Table S1. Annotations for mitochondrial proteins are derived from the 'Integrated Mitochondrial Protein Index' (IMPI), which was downloaded from the MitoMiner database (<http://mitominer.mrc-mbu.cam.ac.uk>; IMPI version Q2 2018; [40]). Only entries for known mitochondrial proteins were considered. Information about components of complex I, IV and V (F₁F₀ ATP synthase) are derived from the Human Genome Organisation (HUGO) Gene Nomenclature Committee (HGNC; <https://www.genenames.org/>; [41])

Radioactive precursor synthesis and *in organello* import

Radiolabeled precursor proteins were synthesized using rabbit reticulocyte lysate (Promega) in the presence of [35S] methionine. The import of radiolabeled precursors into isolated mitochondria was performed at 30°C in import buffer (250 mM sucrose, 80 mM potassium acetate, 5 mM magnesium acetate, 5 mM methionine, 10 mM sodium succinate, 5 mM adenosine triphosphate, and 20 mM HEPES/KOH [pH 7.4]). For TIM22 substrates, import buffer was supplemented with 2 mM ATP, 1 mM DTT, 5 mM creatine phosphate and 0.1 mg/mL

creatine kinase. 2% Lysate was used for TIM23 and MIA40 proteins, whereas 10% was used for TIM22 imported carrier proteins. Samples were incubated with radiolabelled precursors for different times. Import of TIM23 and TIM22 substrates was stopped by the dissipation of membrane potential on ice using 8mM antimycin A, 1 mM valinomycin and 10 mM oligomycin. MIA40 import was stopped by addition of 50 mM IAA and incubation on ice. Non-imported proteins were removed by proteinase K (20µg/mL) treatment for 10 min on ice. PMSF (2 mM) was added to inactivate proteinase K for 10 min on ice. Mitochondria were collected, washed with SEM buffer (250 mM sucrose, 1 mM EDTA, 20 mM Mops [pH 7.2]) and used for SDS-PAGE analyses or BN-PAGE analyses. Results were visualized using digital autoradiography. Quantifications were performed using ImageQuantTL (GE Healthcare) using rolling ball background subtraction.

BN PAGE analyses

Mitochondria were solubilized in buffer containing 1% digitonin (20 mM Tris/HCl [pH 7.4], 0.1 mM EDTA, 50 mM NaCl, 10% (w/v) glycerol and 1 mM PMSF) to a final concentration of 1 mg/mL for 30 min at 4 °C. Lysates were cleared by centrifugation at 14,000g for 15 min at 4 °C and 10x BN loading dye was added (5% Coomassie brilliant blue G-250, 500 mM 6-aminohexanoic acid, and 100 mM Bis-Tris [pH 7.0]). Samples were loaded onto 6%–16% polyacrylamide gradient gels and separated as described [42]

Cysteine modification Assay and Crosslinking

Modification of free thiol groups was performed using the SulfoBiotics Protein Redox State Monitoring Kit Plus (Dojinjo) according to manufacturer's indications with slight modifications. In brief, 200 µg mitochondria were solubilised at 10 µg/ µl using provided detergent for 30 min at 4°C. After clearing samples by centrifugation at

14,000g for 15 min at 4 °C, they were subjected to Cys modification for 30 min at 37°C and subsequently separated by SDS-PAGE. Acrylamide gel was irradiated with UV-light for 15 min and Western blotting was performed afterwards. *In organello* crosslinking was performed using the sulfhydryl crosslinker BMH at 1mM concentration or 1mM CuSO₄ in crosslinker buffer (Sorbitol 0.6 M, 20 mM Hepes [pH 7.2]) for 45 min on ice. Samples were quenched by adding 50 mM Cysteine (for BMH) or 10 mM EDTA and N-ethylmaleimide (NEM) (final concentration). Mitochondria were re-isolated by centrifugation at 10,000xg 10 min at 4°C and subsequently washed with SEM buffer once in the case of BMH crosslinking. Afterwards, FLAG immunoisolation and Western blotting under non-reducing conditions were performed.

FLAG immunoisolation

Isolated mitochondria were solubilized in buffer (50 mM Tris-HCl, [pH 7.4], 150 mM NaCl, 1 mM EDTA, 10% (w/v) glycerol, and 2 mM phenylmethylsulfonyl fluoride [PMSF]) containing 1% (w/v) digitonin (Merck) or 0.2 % triton-x100 (in the case of CuSO₄ crosslinking) and incubated at 4°C. Samples were cleared by centrifugation, and supernatants applied to equilibrated anti-FLAG-agarose (Sigma). After washing, bound proteins were eluted with 1.5x Sample Buffer (94 mM Tris-HCl [pH 6.8], 3% SDS, 25% glycerol, 0.015% Bromophenol Blue) or FLAG peptide and subjected to SDS-PAGE and Western blotting.

Miscellaneous

Standard procedures were used for SDS-PAGE and Western blotting of proteins adsorbed to polyvinylidene fluoride membranes (Millipore). Primary antibodies were raised in rabbit or purchased (COX11, Proteintech. NDUFS1, Proteintech. NDUFS5, Abcam. NDUF8, Abcam. NDUF7, Abcam. NDUF5, Proteintech, COX7A2,

Proteintech. COX3, Proteintech. ATP5O, Proteintech. ATP5F1, Proteintech.). Antigen-antibody complexes were detected by HRP-coupled secondary antibodies and enhanced chemiluminescence detection on X-ray films.

Acknowledgements

We are indebted to M. Balleininger for technical assistance. This work was supported by the Deutsche Forschungsgemeinschaft, the SFB1002 Project A06 (PR), the SFB1190 Project 17 (IB), Project ID 403222702/SFB 1381 (BW), the Excellence Strategy (CIBSS – EXC-2189 – Project-ID 390939984) (BW) as well as the European Research Council ERC335080 (PR) and ERC Consolidator Grant No. 648235 (BW), the Max Planck Society (PR), the Copernicus Award of the Foundation for Polish Science and Deutsche Forschungsgemeinschaft (PR & AC), the Humboldt Foundation (DPG). "Regenerative Mechanisms for Health" project MAB/2017/2, carried out within the International Research Agendas programme of the Foundation for Polish Science co-financed by the European Union under the European Regional Development Fund (AC), National Science Centre, Poland 2015/19/B/NZ3/03272 (MW).

References

- [1] J. Montoya, M.J. López-Pérez, E. Ruiz-Pesini, Mitochondrial DNA transcription and diseases: Past, present and future, *Biochimica Et Biophysica Acta (BBA) - Bioenergetics*. 1757 (2006) 1179–1189. doi:10.1016/j.bbabi.2006.03.023.
- [2] J. Dudek, P. Rehling, M. van der Laan, Mitochondrial protein import: common principles and physiological networks, *Biochim. Biophys. Acta*. 1833 (2013) 274–285.
- [3] D.U. Mick, T.D. Fox, P. Rehling, Inventory control: cytochrome c oxidase assembly regulates mitochondrial translation, *Nat Rev Mol Cell Biol*. 12 (2011) 14–20. doi:10.1038/nrm3029.
- [4] I.C. Soto, F. Fontanesi, J. Liu, A. Barrientos, *Biochimica et Biophysica Acta, BBA - Bioenergetics*. (2011) 1–15. doi:10.1016/j.bbabi.2011.09.005.
- [5] F.-N. Vögtle, J.M. Burkhart, S. Rao, C. Gerbeth, J. Hinrichs, J.-C. Martinou, et

- al., Intermembrane space proteome of yeast mitochondria, *Mol. Cell Proteomics*. 11 (2012) 1840–1852. doi:10.1074/mcp.M112.021105.
- [6] A. Ghosh, P.P. Trivedi, S.A. Timbalia, A.T. Griffin, J.J. Rahn, S.S.L. Chan, et al., Copper supplementation restores cytochrome c oxidase assembly defect in a mitochondrial disease model of COA6 deficiency, *Hum. Mol. Genet.* 23 (2014) 3596–3606. doi:10.1093/hmg/ddu069.
- [7] D. Pacheu-Grau, B. Bareth, J. Dudek, L. Juris, F.-N. Vögtle, M. Wissel, et al., Cooperation between COA6 and SCO2 in COX2 maturation during cytochrome c oxidase assembly links two mitochondrial cardiomyopathies, *Cell Metab.* 21 (2015) 823–833. doi:10.1016/j.cmet.2015.04.012.
- [8] D.A. Stroud, M.J. Maher, C. Lindau, F.-N. Vögtle, A.E. Frazier, E. Surgenor, et al., COA6 is a mitochondrial complex IV assembly factor critical for biogenesis of mtDNA-encoded COX2, *Hum. Mol. Genet.* 24 (2015) 5404–5415. doi:10.1093/hmg/ddv265.
- [9] A. Ghosh, A.T. Pratt, S. Soma, S.G. Theriault, A.T. Griffin, P.P. Trivedi, et al., Mitochondrial disease genes COA6, COX6B and SCO2 have overlapping roles in COX2 biogenesis, *Hum. Mol. Genet.* 25 (2016) 660–671. doi:10.1093/hmg/ddv503.
- [10] M. Bourens, A. Barrientos, Human mitochondrial cytochrome c oxidase assembly factor COX18 acts transiently as a membrane insertase within the subunit 2 maturation module, *J. Biol. Chem.* 292 (2017) 7774–7783. doi:10.1074/jbc.M117.778514.
- [11] S.E. Calvo, A.G. Compton, S.G. Hershman, S.C. Lim, D.S. Lieber, E.J. Tucker, et al., Molecular Diagnosis of Infantile Mitochondrial Disease with Targeted Next-Generation Sequencing, *Science Translational Medicine*. 4 (2012) 118ra10–118ra10. doi:10.1016/j.jmb.2011.10.012.
- [12] F. Baertling, M. A M van den Brand, J.L. Hertecant, A. Al-Shamsi, L. P van den Heuvel, F. Distelmaier, et al., Mutations in COA6 cause cytochrome c oxidase deficiency and neonatal hypertrophic cardiomyopathy, *Hum. Mutat.* 36 (2015) 34–38. doi:10.1002/humu.22715.
- [13] S.C. Leary, F. Sasarman, T. Nishimura, E.A. Shoubridge, Human SCO2 is required for the synthesis of CO II and as a thiol-disulphide oxidoreductase for SCO1, *Hum. Mol. Genet.* 18 (2009) 2230–2240. doi:10.1093/hmg/ddp158.
- [14] S.C. Leary, Human SCO1 and SCO2 have independent, cooperative functions in copper delivery to cytochrome c oxidase, *Hum. Mol. Genet.* 13 (2004) 1839–1848. doi:10.1093/hmg/ddh197.
- [15] S.C. Leary, P.A. Cobine, B.A. Kaufman, G.-H. Guercin, A. Mattman, J. Palaty, et al., The Human Cytochrome c Oxidase Assembly Factors SCO1 and SCO2 Have Regulatory Roles in the Maintenance of Cellular Copper Homeostasis, *Cell Metab.* 5 (2007) 9–20. doi:10.1016/j.cmet.2006.12.001.
- [16] M.N. Morgada, L.A. Abriata, C. Cefaro, K. Gajda, L. Banci, A.J. Vila, Loop recognition and copper-mediated disulfide reduction underpin metal site assembly of Cu AIN human cytochrome oxidase, *Proceedings of the National Academy of Sciences*. 112 (2015) 11771–11776. doi:10.1093/emboj/19.8.1766.
- [17] M. Bourens, A. Boulet, S.C. Leary, A. Barrientos, Human COX20 cooperates with SCO1 and SCO2 to mature COX2 and promote the assembly of cytochrome c oxidase, *Hum. Mol. Genet.* 23 (2014) 2901–2913. doi:10.1093/hmg/ddu003.
- [18] A. Aich, C. Wang, A. Chowdhury, C. Ronsör, D. Pacheu-Grau, R. Richter-Dennerlein, et al., COX16 promotes COX2 metallation and assembly during

- respiratory complex IV biogenesis, *Elife*. 7 (2018). doi:10.7554/eLife.32572.
- [19] S. Maghool, N.D.G. Cooray, D.A. Stroud, D. Aragão, M.T. Ryan, M.J. Maher, Structural and functional characterization of the mitochondrial complex IV assembly factor Coa6, *Life Sci Alliance*. 2 (2019). doi:10.26508/lsa.201900458.
- [20] M. Vukotic, S. Oeljeklaus, S. Wiese, F.-N. Vögtle, C. Meisinger, H.E. Meyer, et al., Rcf1 mediates cytochrome oxidase assembly and respirasome formation, revealing heterogeneity of the enzyme complex, *Cell Metab*. 15 (2012) 336–347. doi:10.1016/j.cmet.2012.01.016.
- [21] A.J. Meyer, T.P. Dick, Fluorescent protein-based redox probes, *Antioxidants & Redox Signaling*. 13 (2010) 621–650. doi:10.1089/ars.2009.2948.
- [22] E. Balatri, L. Banci, I. Bertini, F. Cantini, S. Ciofi-Baffoni, Solution structure of Sco1: a thioredoxin-like protein Involved in cytochrome c oxidase assembly, *Structure*. 11 (2003) 1431–1443.
- [23] Y.-C. Horng, S.C. Leary, P.A. Cobine, F.B.J. Young, G.N. George, E.A. Shoubridge, et al., Human Sco1 and Sco2 function as copper-binding proteins, *J. Biol. Chem*. 280 (2005) 34113–34122. doi:10.1074/jbc.M506801200.
- [24] F. Canonica, D. Klose, R. Ledermann, M.M. Sauer, H.K. Abicht, N. Quade, et al., Structural basis and mechanism for metallochaperone-assisted assembly of the CuA center in cytochrome oxidase, *Sci Adv*. 5 (2019) eaaw8478. doi:10.1126/sciadv.aaw8478.
- [25] L. Banci, I. Bertini, S. Ciofi-Baffoni, I.P. Gerotheranassis, I. Leontari, M. Martinelli, et al., A structural characterization of human SCO2, *Structure*. 15 (2007) 1132–1140. doi:10.1016/j.str.2007.07.011.
- [26] L. Banci, I. Bertini, S. Ciofi-Baffoni, I. Leontari, M. Martinelli, P. Palumaa, et al., Human Sco1 functional studies and pathological implications of the P174L mutant, *Proceedings of the National Academy of Sciences of the United States of America*. 104 (2007) 15–20. doi:10.1073/pnas.0606189103.
- [27] L. Banci, I. Bertini, S. Ciofi-Baffoni, T. Hadjiloi, M. Martinelli, P. Palumaa, Mitochondrial copper(I) transfer from Cox17 to Sco1 is coupled to electron transfer, *Proceedings of the National Academy of Sciences*. 105 (2008) 6803–6808. doi:10.1073/pnas.0800019105.
- [28] S. Soma, M.N. Morgada, M.T. Naik, A. Boulet, A.A. Roesler, N. Dziuba, et al., COA6 Is Structurally Tuned to Function as a Thiol-Disulfide Oxidoreductase in Copper Delivery to Mitochondrial Cytochrome c Oxidase, *Cell Rep*. 29 (2019) 4114–4126.e5. doi:10.1016/j.celrep.2019.11.054.
- [29] N. Denkert, A.B. Schendzielorz, M. Barbot, L. Versemann, F. Richter, P. Rehling, et al., Cation selectivity of the presequence translocase channel Tim23 is crucial for efficient protein import, *Elife*. 6 (2017). doi:10.7554/eLife.28324.
- [30] A. Geissler, A. Chacinska, K.N. Truscott, N. Wiedemann, K. Brandner, A. Sickmann, et al., The mitochondrial presequence translocase: an essential role of Tim50 in directing preproteins to the import channel, *Cell*. 111 (2002) 507–518. doi:10.1016/s0092-8674(02)01073-5.
- [31] C. Schulz, O. Lytovchenko, J. Melin, A. Chacinska, B. Guiard, P. Neumann, et al., Tim50's presequence receptor domain is essential for signal driven transport across the TIM23 complex, *J Cell Biol*. 195 (2011) 643–656. doi:10.1073/pnas.1014918108.
- [32] D. Brancaccio, A. Gallo, M. Piccioli, E. Novellino, S. Ciofi-Baffoni, L. Banci, [4Fe-4S] Cluster Assembly in Mitochondria and Its Impairment by Copper, *J.*

- Am. Chem. Soc. 139 (2017) 719–730. doi:10.1021/jacs.6b09567.
- [33] S. Callegari, T. Müller, C. Schulz, C. Lenz, D.C. Jans, M. Wissel, et al., A MICOS-TIM22 Association Promotes Carrier Import into Human Mitochondria, *Journal of Molecular Biology*. 431 (2019) 2835–2851. doi:10.1016/j.jmb.2019.05.015.
- [34] S. Dennerlein, A. Rozanska, M. Wydro, Z.M.A. Chrzanowska-Lightowlers, R.N. Lightowlers, Human ERAL1 is a mitochondrial RNA chaperone involved in the assembly of the 28S small mitochondrial ribosomal subunit, *Biochem. J.* 430 (2010) 551–558. doi:10.1042/BJ20100757.
- [35] D. Pacheu-Grau, A. Gómez-Durán, E. López-Gallardo, T. Pinós, A.L. Andreu, M.J. López-Pérez, et al., “Progress” renders detrimental an ancient mitochondrial DNA genetic variant, *Hum. Mol. Genet.* 20 (2011) 4224–4231. doi:10.1093/hmg/ddr350.
- [36] M. Lazarou, D.R. Thorburn, M.T. Ryan, M. McKenzie, Assembly of mitochondrial complex I and defects in disease, *Biochim. Biophys. Acta.* 1793 (2009) 78–88. doi:10.1016/j.bbamcr.2008.04.015.
- [37] K. Mohanraj, M. Wasilewski, C. Benincá, D. Cysewski, J. Poznanski, P. Sakowska, et al., Inhibition of proteasome rescues a pathogenic variant of respiratory chain assembly factor COA7, *EMBO Mol Med.* 11 (2019). doi:10.15252/emmm.201809561.
- [38] J. Cox, M. Mann, MaxQuant enables high peptide identification rates, individualized p.p.b.-range mass accuracies and proteome-wide protein quantification, *Nature Biotechnology.* 26 (2008) 1367–1372. doi:10.1038/nbt.1511.
- [39] J. Cox, N. Neuhauser, A. Michalski, R.A. Scheltema, J.V. Olsen, M. Mann, Andromeda: a peptide search engine integrated into the MaxQuant environment, *J. Proteome Res.* 10 (2011) 1794–1805. doi:10.1021/pr101065j.
- [40] A.C. Smith, A.J. Robinson, MitoMiner v4.0: an updated database of mitochondrial localization evidence, phenotypes and diseases, *Nucleic Acids Research.* 47 (2019) D1225–D1228. doi:10.1093/nar/gky1072.
- [41] B. Braschi, P. Denny, K. Gray, T. Jones, R. Seal, S. Tweedie, et al., Genenames.org: the HGNC and VGNC resources in 2019, *Nucleic Acids Research.* 47 (2019) D786–D792. doi:10.1093/nar/gky930.
- [42] I. Wittig, H.-P. Braun, H. Schagger, Blue native PAGE, *Nature Protocols.* 1 (2006) 418–428. doi:10.1038/nprot.2006.62.

Figure Legends

Figure 1. Lack of COA6 affects complex I and complex IV

A. Scheme of COA6 function in copper transfer to Cu_A center in COX2 (IMS, intermembrane space). **B** Cell were seeded in glucose containing medium to equal density and counted after 72h. Cell numbers were calculated and are presented as % of wild type (WT) (mean \pm SEM, n= 3). **C.** Representative real-time respirometry analysis of intact cells. Values are presented as mean \pm SEM, n=6. **D.** Activity of complex IV (mOD/min) was measured photometrically; (mean \pm SEM, n= 3). **E** Complex IV amount was measure by ELISA (mean \pm SEM, n= 3). **F.** Complex I activity (mOD/min) was measured photometrically; (mean \pm SEM, n= 3). **G.** Reactive oxygen species in wild type (WT) and COA6 knock out cells (COA6^{KO}) cells were assessed by MitoSOX staining and flow cytometry; (mean \pm SEM, n= 3). **H.** Glutathione redox potentials were measured in wild type (WT) and COA6 knock out cells upon transfection with either Mito-Grx1-roGFP2 or IMS-Grx1-roGFP2 and analyzed by live imaging. Ratio of fluorescence at 405/470 nm is presented as average \pm SEM, n>44.

Figure 2. Lacks of COA6 impacts protein import.

A. Quantitative MS analysis of changes in the mitochondrial proteome in cells lacking COA6. **B.** Purified wild type (WT) and COA6^{KO} mitochondria were analyzed by SDS-PAGE and Western blotting. **C.** Mitochondrial membrane potential was measured by flow cytometry using the dye JC-1. Fluorescence signals are depicted as mean \pm SEM, n= 4. **D.** *In vitro* import of radiolabeled precursor proteins into purified wild type (WT) and COA6^{KO} mitochondria. Su9-DFHR and OTC were imported for indicated times in the presence or the absence of membrane potential ($\Delta\psi$). Samples were

Proteinase K (PK) treated after import, subjected to SDS-PAGE, and proteins visualized by digital autoradiography (p, precursor; m, mature). **E.** Quantification of Su9-DFHR import into mitochondria. Signals were quantified and are presented as percent of the longest import timepoint in the wild type (WT) sample, mean, SEM +/- SEM, n=3. **F.** *In vitro* import of radiolabeled carrier precursors ANT3 (ADP/ATP carrier 3) and SLC25A19 (thiamine pyrophosphate carrier) into purified wild type (WT) and COA6^{KO} mitochondria. Import was carried out for different times in the presence or absence of $\Delta\psi$. After import mitochondria were proteinase K (PK) treated, solubilized, and subjected to BN-PAGE separation and digital autoradiography. **G.** Quantification of ANT3 import into mitochondria. Signals were quantified and are presented as percent of the longest import timepoint in the wild type (WT) sample, mean, SEM +/- SEM, n=3. **H.** *In vitro* import of radiolabeled twin CX_NC motifs containing precursors COX6B1 and COX19 into purified wild type (WT) and COA6^{KO} mitochondria. Import was carried out for indicated times in the presence or absence of the cysteine modifying agent iodoacetamide (IA). Samples were subjected to proteinase K (PK) digested and analyzed by SDS-PAGE and digital autoradiography. **I.** Quantification of COX6B1 import into mitochondria. Signals were quantified and are shown as percent of the longest import timepoint in the wild type (WT) sample; mean, SEM +/- SEM, n=3.

Figure 3. Cysteines in the CXXXC motif of SCO2 are required for binding to COA6

A. Wild type (WT) and COA6^{FLAG} mitochondria were subjected to chemical crosslinking using the homo-bifunctional crosslinker BMH. After crosslinking, mitochondria were solubilized and subjected to anti-FLAG immunisolation. Samples were analyzed by SDS-PAGE and Western blotting. **B.** Schematic representation of

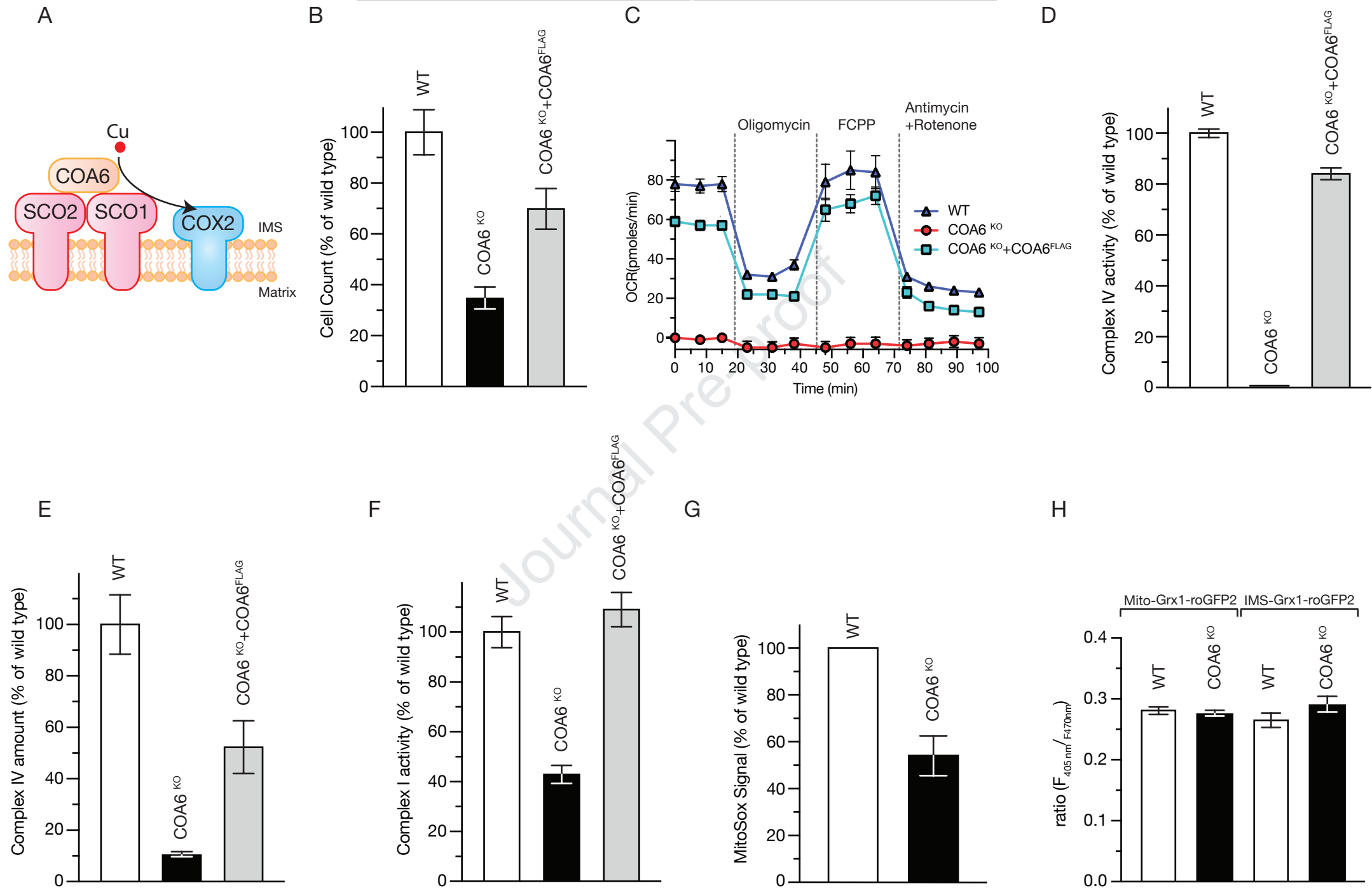
generated SCO2 mutants. Red, cysteines of the CX₃X_NH motif; Green, ex-changed residue; TM, transmembrane span. **C** *In vitro* import of radiolabeled SCO2^{WT} into purified wild type mitochondria in presence or the absence of membrane potential ($\Delta\psi$). Samples were subjected to proteinase K (PK) digest, and analyzed by SDS-PAGE and digital autoradiography. **D**. *In vitro* import of SCO2 cysteine mutants as in C. **E**. After *in vitro* import of indicated SCO2 variants into purified wild type (WT) and COA6^{FLAG} mitochondria, samples were solubilized, subjected to anti FLAG immunoisolation, and eluates analyzed by SDS-PAGE, digital autoradiography and Western blotting. **F**. Wild type (WT) and COA6^{FLAG} mitochondria were subjected to CuSO₄ treatment. After treatment, mitochondria were solubilized and subjected to anti-FLAG immunisolation. Samples were analyzed by SDS-PAGE and Western blotting. **G**. SCO1^{FLAG} immunoisolation after *in vitro* import of SCO2 variants into purified wild type (WT) and SCO1^{FLAG} mitochondria. After import of radiolabeled SCO2 variants, anti FLAG immunoisolation was performed and eluates analyzed by SDS-PAGE and digital autoradiography.

Figure 4. COA6 acts as a thiol-reductase for copper metallochaperones SCO1 and SCO2

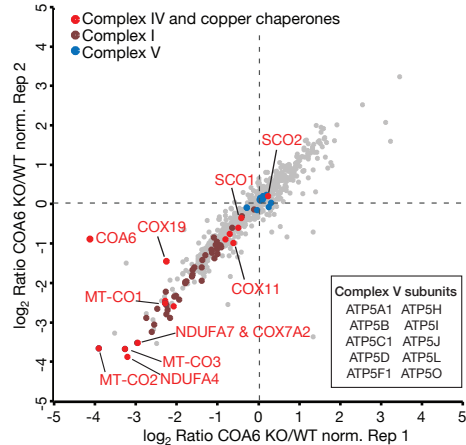
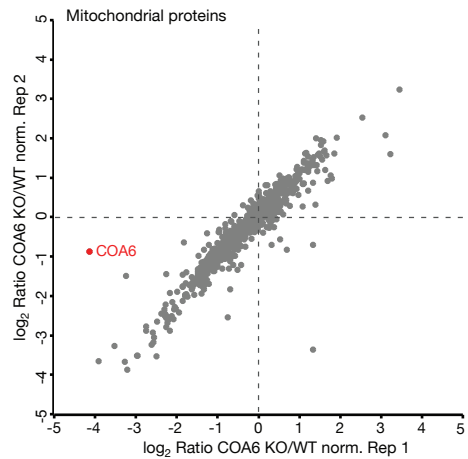
A. Wild type (WT) and COA6^{KO} mitochondria were incubated in the presence or absence of DTT and subjected to cysteine modification. Samples were subjected to SDS-PAGE and western blotting. **B**. Quantification of the ratio between most reduced and most oxidized form of SCO2 in wild type (WT) and COA6^{KO} mitochondria presented as percent of WT; mean +/- SEM, n=3 **C and D**. Cysteine redox modification assay for SCO1 was carried out as described in A and B. **E and F**. Cysteine redox modification assay for SCO2 and SCO1 in cells expressing

COA6^{FLAG}. Wild type (WT) COA6^{KO} and COA6^{KO}+COA6^{FLAG} mitochondria were subjected cysteine modification and analyzed by SDS-PAGE and western blotting.

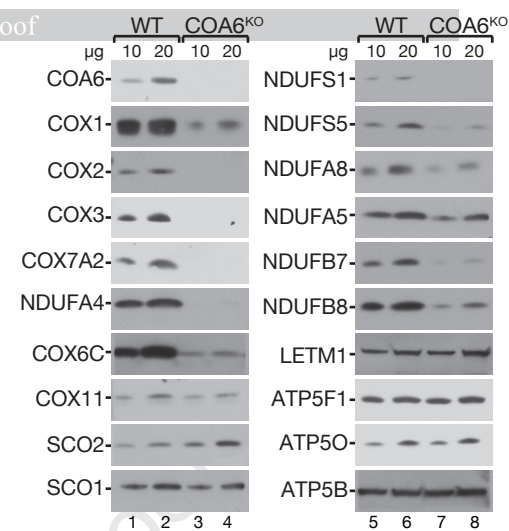
Journal Pre-proof



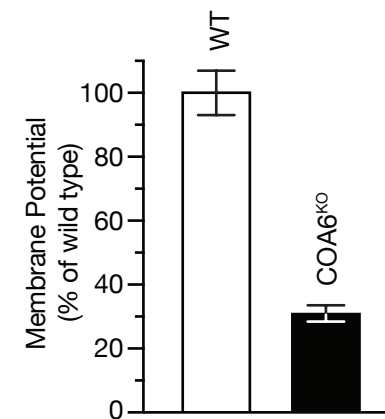
A



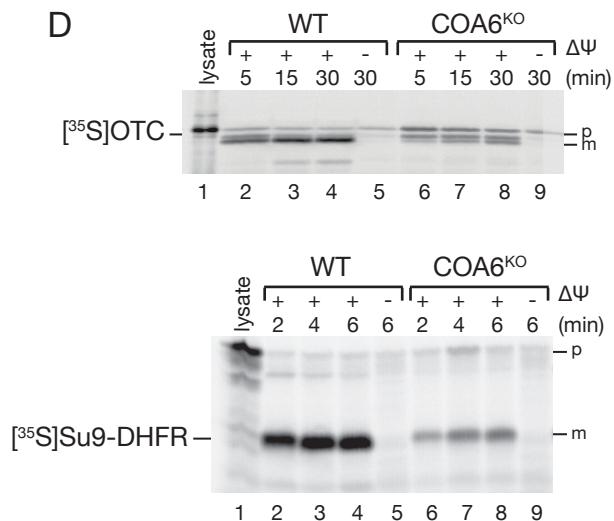
Journal Pre-proof



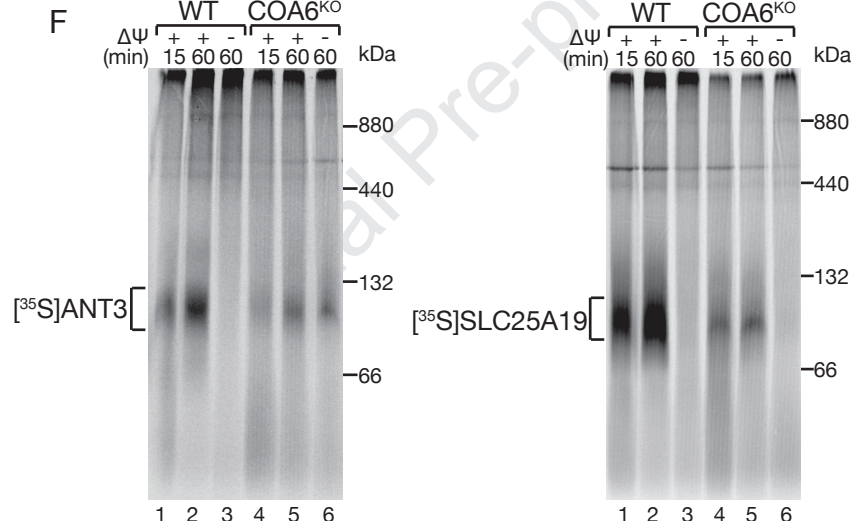
C



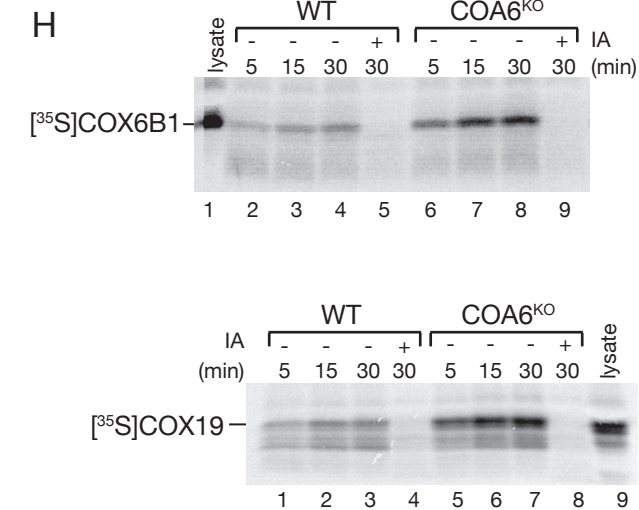
D



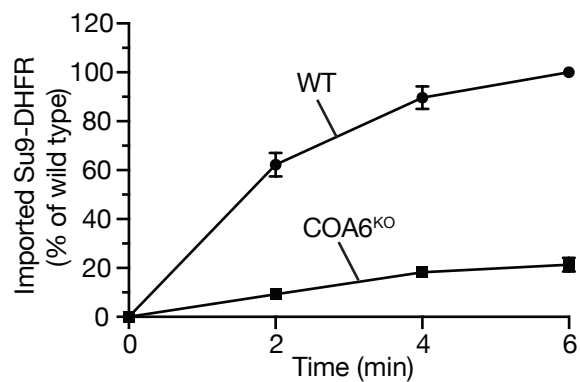
F



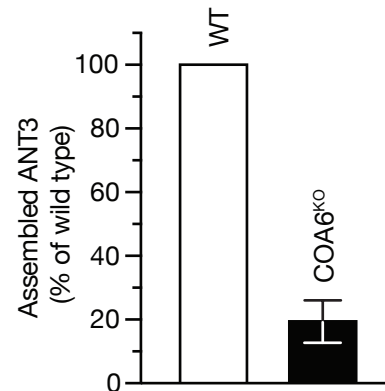
H



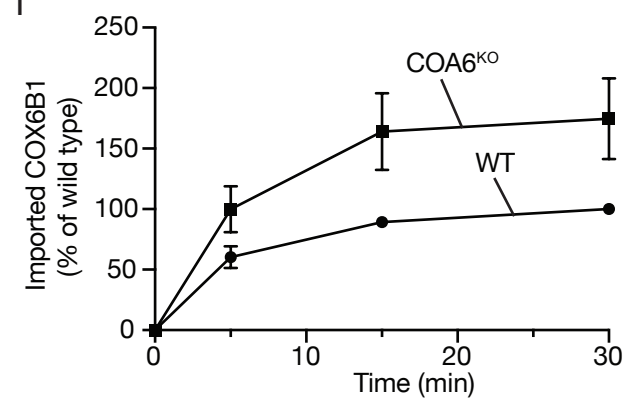
E

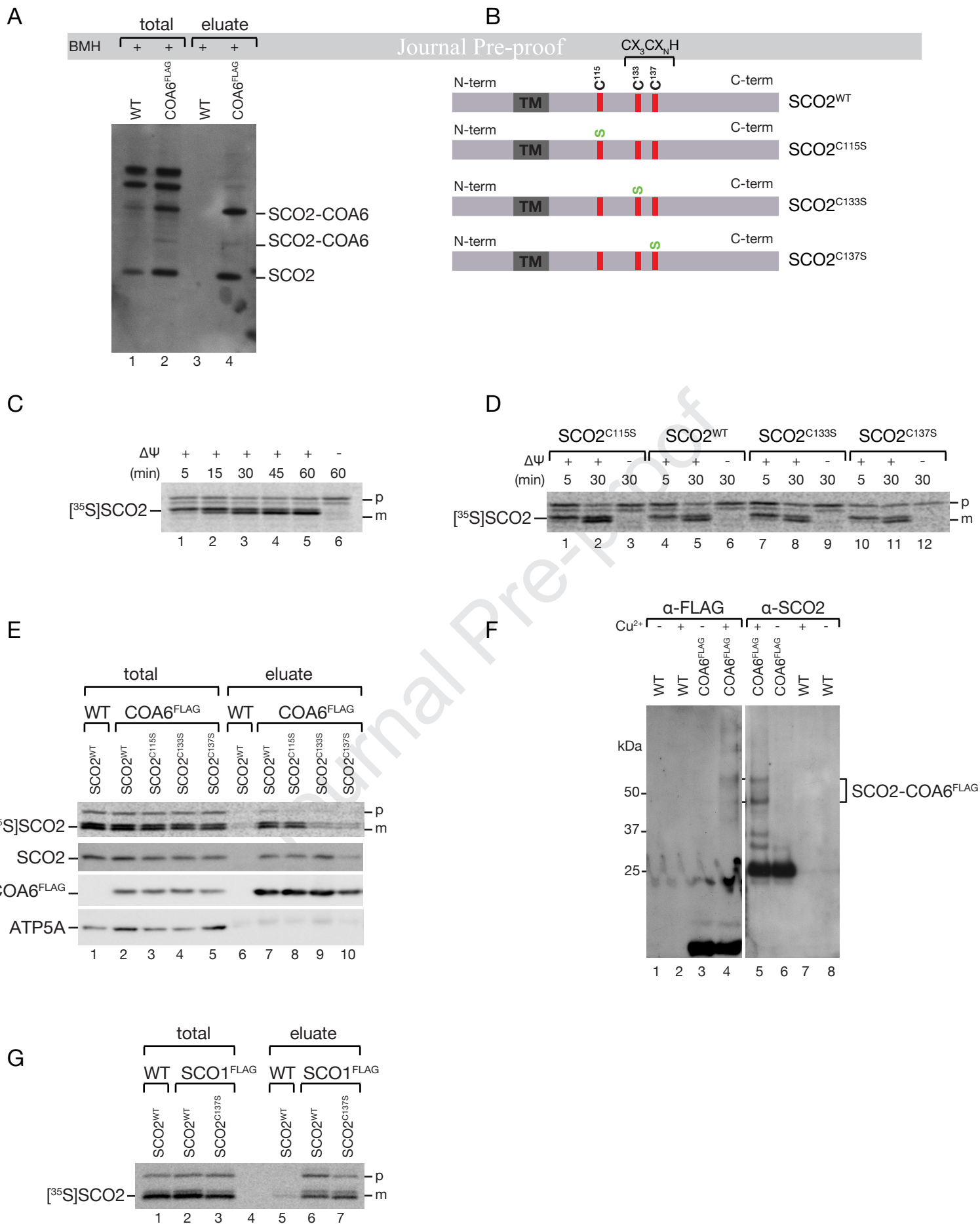


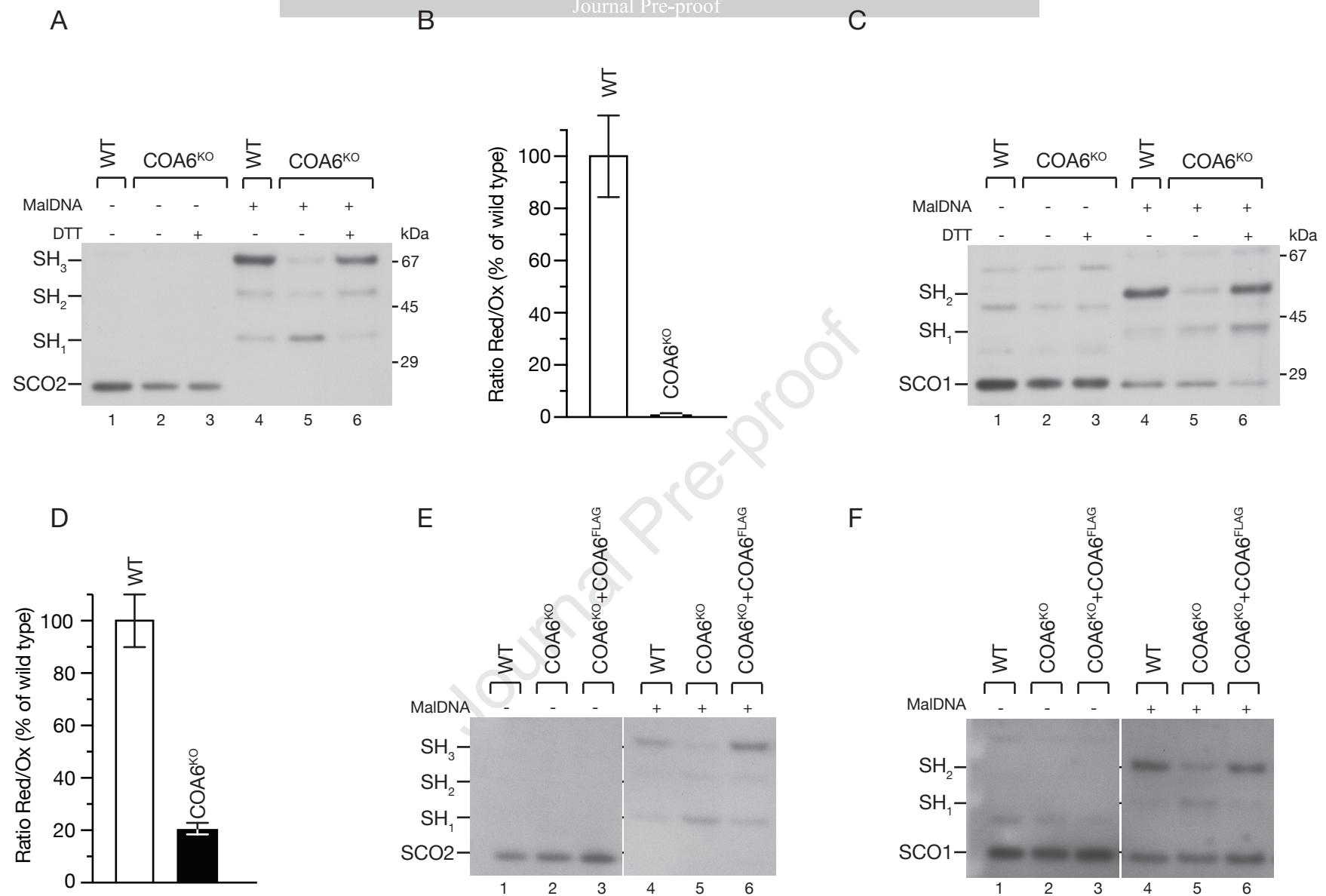
G



I







- Loss of COA6 affects respiratory chain complexes IV and I.
- Decreased membrane potential driven protein import due to loss of COA6.
- Cysteine residues in CX₃CX_NH motif of SCO2 mediate COA6 interaction.
- COA6 acts as thiol reductase for copper metallochaperones during Cu_A biogenesis.

Journal Pre-proof